

**Master's Thesis**

Title

**An Available Bandwidth Measurement Method  
for Arbitrary Parts of End-to-End Path**

Supervisor

**Professor Masayuki Murata**

Author

**Kazumasa Koitani**

February 12th, 2013

Department of Information Networking  
Graduate School of Information Science and Technology  
Osaka University

Master's Thesis

An Available Bandwidth Measurement Method  
for Arbitrary Parts of End-to-End Path

**Kazumasa Koitani**

**Abstract**

The available bandwidth on an end-to-end network path is an important metric for detecting network congestion, adapting transmission rate, configuring paths and topologies on overlay networks, and so on. The existing available bandwidth measurement techniques aimed only at knowing available bandwidth of bottleneck part on the path and most of them do not specify where the bottleneck is. Also, they cannot measure available bandwidth of multiple parts on the path separately. If we can know available bandwidth of each part of the path, we, for example, can rapidly configure the path on the overlay network to satisfy performance requirements of application services. Also, in wireless-cum-wired network environment, we can improve data rate selection on the wireless network dependent on the network resource amount of the wired network. However, to the best of our knowledge, there is no existing works on simultaneous measurement of multiple parts of a network path in an end-to-end fashion.

In this thesis, we propose a simultaneous measurement method of available bandwidth of multiple parts on an end-to-end network path. The proposed method adapts an end-to-end measurement principle, and estimates available bandwidth based on changes in packet sending and arrival intervals under the situation where intermediate routers can record arriving and departing times on incoming packets as a timestamps. Specifically, considering the effect of cross traffic on traversing networks, the endhost sends probe packets at various rates and estimates the available bandwidth using their incoming and outgoing rates based on statistical processing using fluid traffic model. We present extensive simulation results of the proposed method and confirm that it can accurately measure available bandwidth of each part on the path even when the available bandwidth of the sender-side network is smaller than that of the receiver-side network. We also evaluate the proposed method with numerous network scenarios varying physical and available bandwidth settings, hop count of the path, and confirm the robustness of the proposed method.

**Keywords**

Available Bandwidth

Physical Bandwidth

Active Probing

Simultaneous Measurement

Timestamp

# Contents

<b>1</b>	<b>Introduction</b>	<b>6</b>
<b>2</b>	<b>End-to-End Measurement of Available Bandwidth</b>	<b>8</b>
2.1	Definition of Available Bandwidth . . . . .	8
2.2	Existing Methods and Their Limitations . . . . .	9
<b>3</b>	<b>Multiple-Part Measurement of Available Bandwidth</b>	<b>10</b>
3.1	Feasibility of Multiple-Part Measurement . . . . .	10
3.2	Proposed Method . . . . .	16
3.2.1	Overview . . . . .	16
3.2.2	Hop-by-Hop Timestamp of Probe Packets . . . . .	16
3.2.3	Calculation of Available Bandwidth Based on Statistical Processing . . . . .	17
<b>4</b>	<b>Performance Evaluation</b>	<b>19</b>
4.1	Fundamental Evaluation of the Proposed Method . . . . .	19
4.2	Influence of Physical Bandwidth . . . . .	20
4.3	Influence of Hop Count of a Path . . . . .	20
4.4	Performance in multiple bottleneck situation . . . . .	34
<b>5</b>	<b>Conclusion and Future Work</b>	<b>35</b>
	<b>Acknowledgments</b>	<b>36</b>
	<b>Reference</b>	<b>37</b>

## List of Figures

1	Network model . . . . .	9
2	Network model for multiple-part measurement on the path . . . . .	11
3	Network topology for simulation experiments in Subsection 3.1 . . . . .	11
4	Relationship between incoming and outgoing rates with $X_1 = 30$ and $X_2 = 70$ .	12
5	Relationship between incoming and outgoing rates with $X_1 = 50$ and $X_2 = 40$ .	13
6	Relationship between incoming and outgoing rates with $X_1 = 50$ and $X_2 = 30$ .	14
7	Computation of available bandwidth in the proposed method . . . . .	17
8	Estimation results with 100 [Mbps] of physical bandwidth . . . . .	21
9	Estimation results with 10 [Mbps] of physical bandwidth . . . . .	22
10	Estimation results with 1 [Gbps] of physical bandwidth . . . . .	23
11	3 hop network topology . . . . .	24
12	Estimation results with 3 hop topology when $A(1) = 10$ [Mbps] . . . . .	25
13	Estimation results with 3 hop topology when $A(1) = 30$ [Mbps] . . . . .	26
14	Estimation results with 3 hop topology when $A(1) = 50$ [Mbps] . . . . .	27
15	Estimation results with 3 hop topology when $A(1) = 70$ [Mbps] . . . . .	28
16	Estimation results with 3 hop topology when $A(1) = 90$ [Mbps] . . . . .	29
17	Network topologies with longer hop counts . . . . .	31
18	Effect of hop count in scenario 1 . . . . .	32
19	Effect of hop count in scenario 2 . . . . .	33
20	Estimation results in multiple bottleneck situation . . . . .	34

## List of Tables

1	Settings of available bandwidth in 3, 5, and 9 hop topologies . . . . .	31
---	---	----

# 1 Introduction

The amount of the Internet traffic is rapidly increasing [1] due to recent wide spread of IP-reachable devices including smartphones, tablets, laptop PCs. Also, various technologies for access and backbone networks are emerging, that makes the structure of the Internet more complex and heterogeneous. In such environment, bandwidth-related information on an end-to-end network path is quite important for assuring the quality of network application. Especially, the available bandwidth on an end-to-end network path is an important metric for detecting network congestion [2], adapting transmission rate, configuring paths and topologies on overlay networks [3], and so on. For example, if the endhosts know a path is congested, the endhost can set the transmission rate on the path to lower, which makes end-to-end packet delay and loss lower. On the other hand, in general, the available bandwidth largely fluctuates [4] due to various network factors such as congestion. However, due to the current protocol structure of the Internet, applications on an end-host cannot be explicitly notified of bandwidth-related information from the network. Therefore, it is important to obtain bandwidth-related information on end-to-end network paths by conducting measurement at endhosts.

The available bandwidth on an end-to-end network path is determined by a bottleneck part, which has the smallest available bandwidth of the path. Many existing tools for measuring available bandwidth of an end-to-end network path are proposed [3, 5–33]. These tools can obtain a value of available bandwidth at bottleneck part, but it cannot determine where is the bottleneck part on the path except a tool *pathneck* [20], which specify the bottleneck part on the path. Also, they do not measure available bandwidth of each part of the path separately, while knowing the bottleneck location may enhance the quality of network applications. For example, we assume that an endhost use a realtime application, such as video and voice conference [34, 35], which constructs an overlay network. When an endhost determines the location of bottleneck link by bandwidth measurement, the endhost can enhance the quality of network services by adding or deleting the overlay node to the overlay network to change the route of the path between endhosts. Another example is the network control in a wired-cum-wireless network environment. We assume that an end-to-end network path consists of a wireless network part and a wired network part and a sender-side endhost connects to wireless network. When the sender-side endhost finds that the bottleneck locates at the wired network, it can configure the data rate of the wireless network

to lower bit rate which has more robustness against the channel error, which enhances the quality of the network application. However, according to our knowledge, there is no previous research on such end-to-end measurement of available bandwidth of multiple parts of the network path.

In this thesis, we propose a simultaneous measurement method of available bandwidth of multiple parts on an end-to-end network path. The proposed method estimates available bandwidth based on the assumption that some of intermediate routers on the path can record arriving and departing times of traversing packets as timestamps. We divide the end-to-end path into multiple parts by such intermediate routers and estimate the available bandwidth of each part of the path simultaneously, by observing intervals of incoming and outgoing packets on each network. Considering the effect of cross traffic on traversing networks, the endhost sends probe packets at various rates and estimates the available bandwidth based on their incoming and outgoing rates at each part of the path. For the estimation of available bandwidth, we construct a simple mathematical model of the relationships between incoming and outgoing rates of packets.

To evaluate the performance of the proposed method, we conduct simulation experiments using ns-2 [36]. We evaluate the measurement accuracy of the proposed method in various bandwidth settings including situations where the available bandwidth of the sender-side network is smaller than that of the receiver-side network. We also evaluate the proposed method with numerous network scenarios varying physical and available bandwidth settings, hop count of the path, and confirm the robustness of the proposed method.

The rest of this thesis is organized as follows. Section 2 describes a principle of end-to-end available bandwidth measurement based on the existing method. Section 3 adapts this principle to multiple-parts measurement and verifies its feasibility. After that, we propose a multiple-part measurement method of available bandwidth. Section 4 evaluates the measurement accuracy of the proposed method in various situations. In Section 5, we conclude this thesis and describe future work.

## 2 End-to-End Measurement of Available Bandwidth

In this section, we explain a fundamental principle of measurement of the available bandwidth on an end-to-end network path. There are many existing tools for measuring end-to-end available bandwidth such as Cprobe [5], Pathload [6], pathChirp [7]. In these methods, a sender generates probe packets and sends them to a receiver at a certain rate. The receiver observes arrival intervals of probe packets, and determines whether or not sending rate of probe packets from the sender is larger than the available bandwidth of the path between the sender and the receiver, by comparing sending and arrival intervals of the probe packets. Many of existing tools repeats this behavior with various sending rates to determine the available bandwidth accurately. In what follows in this section, we briefly explain the mathematical background of the above methods.

### 2.1 Definition of Available Bandwidth

We assume that the network model in this section is depicted in Figure 1 and the path between the sender and the receiver is already determined and is not varied. The probe packets are sent from the sender to the receiver while the routers on the path hold the probe packets in the buffer and send to the receiver. The path consists of  $H$  links, and each of which is denoted as link  $i$  ( $1 \leq i \leq H$ ). The physical bandwidth of the link  $i$  is denoted as  $C_i$ . The physical bandwidth  $C$  on an end-to-end network path is equal to that of the narrowest link, and it is represented as follows.

$$C \equiv \min_{1 \leq i \leq H} C_i \quad (1)$$

The average bandwidth utilization of link  $i$  at time  $t$  is denoted as  $u_i(t)$ . Then, the available bandwidth of link  $i$  at time  $t$ , denoted by  $A_i(t)$ , is represented as follows.

$$A_i(t) \equiv C_i(1 - u_i(t)) \quad (2)$$

The available bandwidth on an end-to-end network path is equal to that of the link which has smallest available bandwidth. Thus, the available bandwidth on the path at time  $t$  is represented as follows.

$$A(t) \equiv \min_{1 \leq i \leq H} C_i(1 - u_i(t)) \quad (3)$$

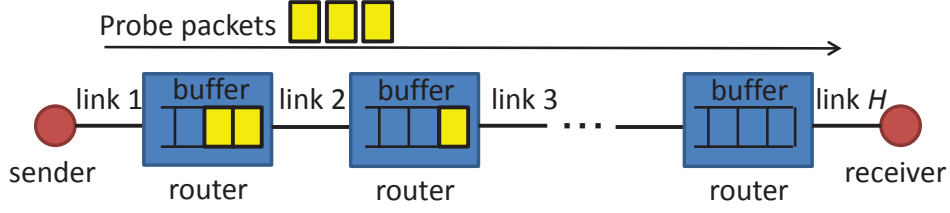


Figure 1: Network model

## 2.2 Existing Methods and Their Limitations

We next explain a principle of available bandwidth on an end-to-end network path. It exploits the relationships between one-way delay from the sender to the receiver and sending and arrival intervals of probe packets.

The sender sends a sequence of  $K$  probe packets to the receiver. The sending time of  $k$  th ( $1 \leq k \leq K$ ) probe packet from the sender is denoted as  $t_k$ , and the arrival time of the packet at the receiver is denoted as  $t'_k$ . The one-way delay of  $k$  th probe packet is represented as  $D_k = t'_k - t_k$ . We focus on the difference between one-way delays of  $k$  th and  $(k + 1)$  th probe packets as follows.

$$\begin{aligned}
 \Delta D_k &= D_{k+1} - D_k \\
 &= (t'_{k+1} - t_{k+1}) - (t'_k - t_k) \\
 &= (t'_{k+1} - t'_k) - (t_{k+1} - t_k) \\
 &= \Delta t'_k - \Delta t_k
 \end{aligned} \tag{4}$$

$\Delta t'_k$  in Equation (4) is an arrival interval of  $k$  th and  $(k + 1)$  th probe packets at the receiver, and  $\Delta t_k$  is a sending interval of the corresponding packets. When the sending rate of probe packets is larger than the available bandwidth, the value of Equation (4) becomes positive since the arrival intervals become larger than the sending intervals. On the other hand, when the sending rate at the sender is equal to or smaller than the available bandwidth, the value of Equation (4) is roughly equal to 0 since we can expect the interval of packets remains unchanged when passing through the network. Note that we do not require the synchronization of clocks at senders and receivers to evaluation Equation (4), while the measurement of one-way delay requires it.

Therefore, by sending probe packets at a certain rate and observing their arrival at the receiver, we can determine whether the sending rate is larger than available bandwidth or not. Repeating these operations enables the estimation of available bandwidth on an end-to-end network path.

### 3 Multiple-Part Measurement of Available Bandwidth

In this section, we propose a simultaneous measurement method of multiple parts on an end-to-end network path by extending the principle described in Section 2.

We assume that a network path between a sender and a receiver is divided into multiple parts by intermediate routers, as depicted in Figure 2. Each part of the path from the sender is called as 1st network section, 2nd network section, ...,  $N$  th network section. The physical bandwidth of  $j$  th network section is denoted as  $C(j)$ , and the available bandwidth is denoted as  $A(j)$ , assuming that the physical bandwidth and the available bandwidth of each network section remains unchanged during a measurement task. We focus on measuring the available bandwidth for all network sections by using probe packets sent from the sender to the receiver.

#### 3.1 Feasibility of Multiple-Part Measurement

Measuring available bandwidth of a single network section can be conducted by injecting probe packets into the network section with various rates, which should be both larger and smaller than the actual available bandwidth of the network section. When all of the injecting rates of all probe packets are smaller than the actual available bandwidth, we cannot measure the available bandwidth accurately. Therefore, to measure the available bandwidth of all network sections on the path, one can consider the following condition needs to be satisfied.

$$\min_{1 \leq k < j} A(k) > A(j) \quad (1 \leq j \leq N) \quad (5)$$

Conversely, measuring available bandwidth is impossible when the available bandwidth of  $j$  th network section is smaller than that of  $(j+1)$  th network section. This is inspired by the expectation that the rate at which probing packets going out of a certain network section would be equal to or smaller than the available bandwidth of the section. However, when the probing packets are injected at enough high rates, the outgoing rate would become larger than the actual available bandwidth of the network section [37]. This means that there is a feasibility of measuring the available bandwidth of network sections even when Equation (5) is not satisfied. In what follows, we validate the feasibility by simulation experiments using ns-2.

Figure 3 shows the network topology used in the simulation experiments. The propagation delay of the link between n4 and n5 (we call it the *first link*) and that between n5 and n6 (the

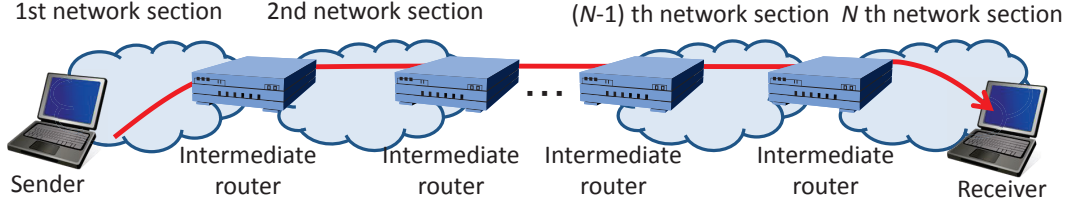


Figure 2: Network model for multiple-part measurement on the path

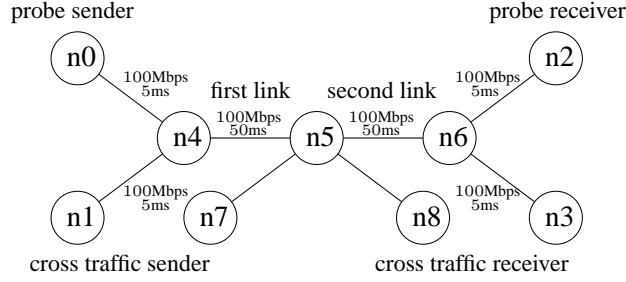


Figure 3: Network topology for simulation experiments in Subsection 3.1

*second link*) is 50 [ms]. Other links have 5 [ms] delay. The physical bandwidth of all links in the network is 100 [Mbps]. Cross traffic is sent from node n1 to node n8 via nodes n4 and n5 at  $X_1$  [Mbps]. Another cross traffic is sent from node n7 to node n3 via nodes n5 and n6 at  $X_2$  [Mbps]. Therefore, the available bandwidth of the first link is  $(100 - X_1)$  [Mbps], and that of the second link is  $(100 - X_2)$  [Mbps]. The cross traffic is constructed from UDP packets whose sending intervals follows the exponential distribution with designated mean value. Probe packets are sent from node n0 to node n2 via nodes n4, n5, and n6, traversing the first and second links. The intervals of probe packets sent from node n0 is varied from  $1.0 \times 10^{-4}$  [s] to  $2.0 \times 10^{-3}$  [s] in units of  $1.0 \times 10^{-5}$  [s], which corresponds to the rate from 6 [Mbps] to 120 [Mbps]. The number of probe packets sent at a time is  $K$ . The probe packet size is set to 1500 [Bytes] and the packet size of cross traffic is set to 1000 [Bytes]. Under these settings, we observe incoming and outgoing rates of probe packets at the second link. We utilize the average rate of  $K_0$  probe packets as the incoming and outgoing rates.

Figures 4, 5, and 6 show the simulation results, where we plot the relationship between incoming and outgoing rates of probe packets at the second link when  $K_0 = 2, 6,$  and  $10$ . Figure 4 plots the results when  $X_1 = 30$  and  $X_2 = 70$ . In the case, the actual value of the available bandwidth

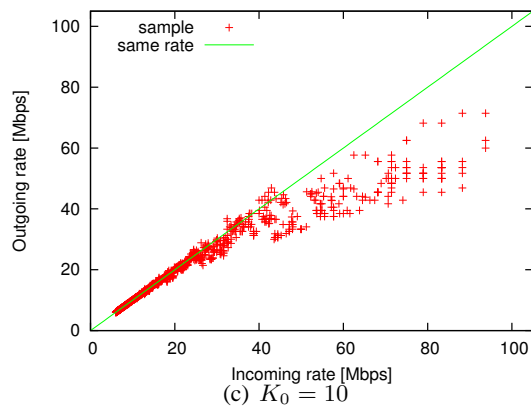
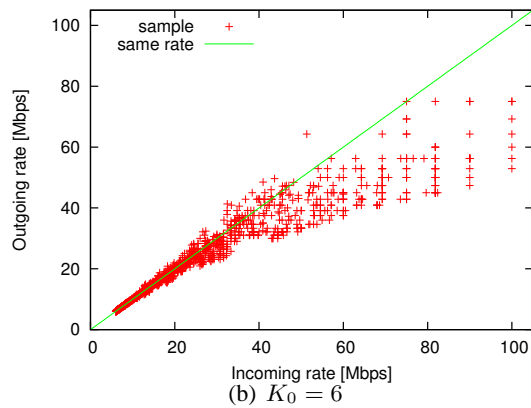
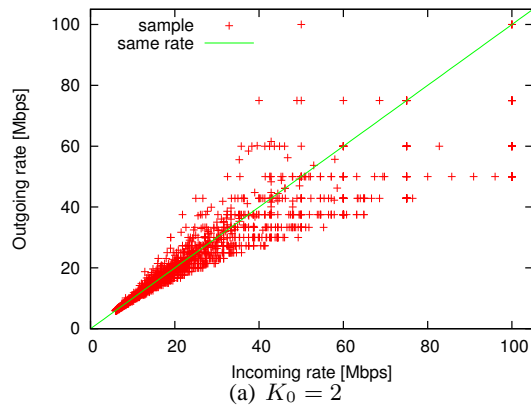


Figure 4: Relationship between incoming and outgoing rates with  $X_1 = 30$  and  $X_2 = 70$

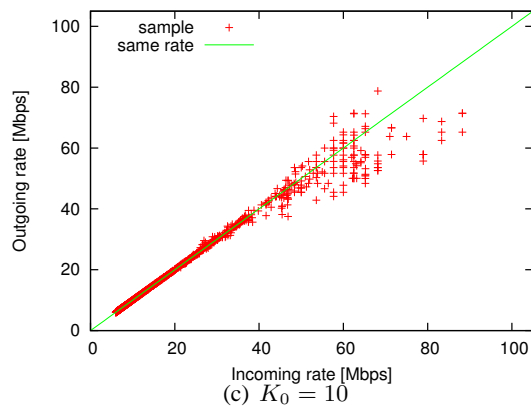
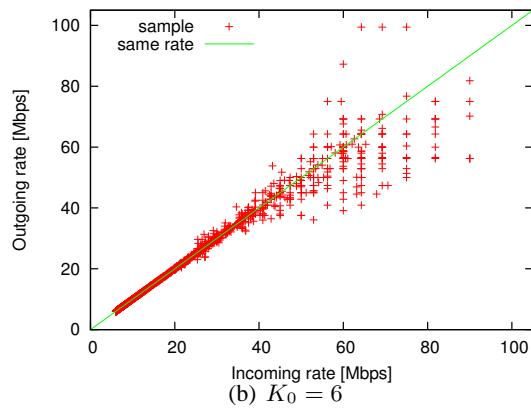
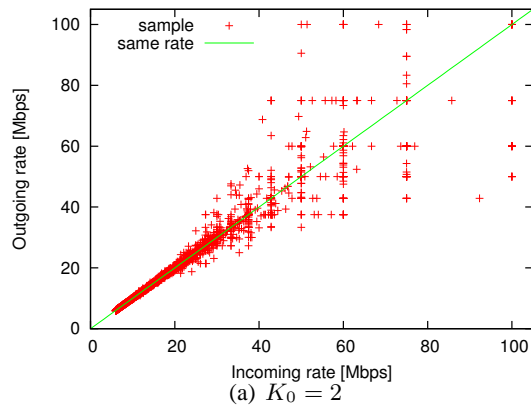


Figure 5: Relationship between incoming and outgoing rates with  $X_1 = 50$  and  $X_2 = 40$

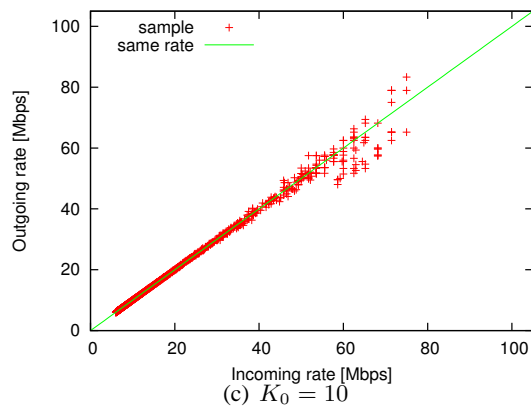
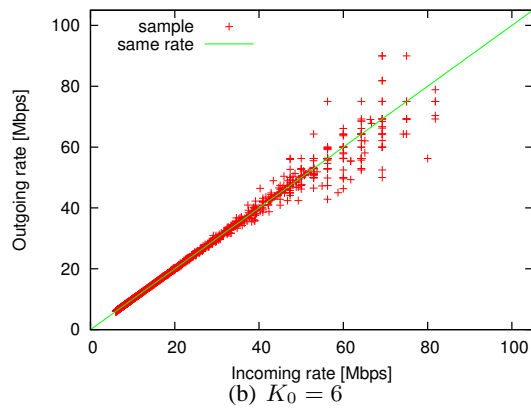
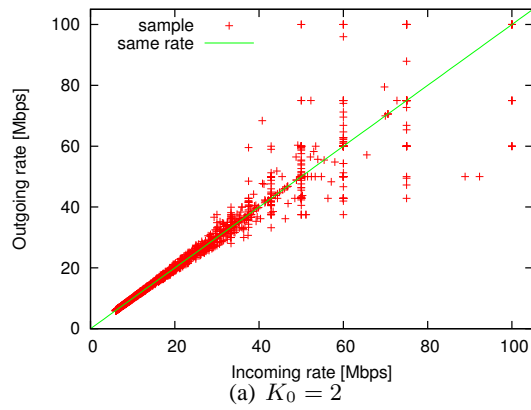


Figure 6: Relationship between incoming and outgoing rates with  $X_1 = 50$  and  $X_2 = 30$

at the second link is 30 [Mbps], which is smaller than that of the first link (70 [Mbps]) and Equation (5) is satisfied. Therefore, we expect the available bandwidth measurement of second link can be done easily. This can be confirmed by Figure 4 where the incoming rate varies from small values to large values close to 100 [Mbps], and that when the incoming rate is large, the outgoing rate becomes smaller than the incoming rate.

Figure 5 show the case where  $X_1 = 50$  and  $X_2 = 40$ . Since the actual available bandwidth of the first and second links is 50 and 60 [Mbps], respectively, Equation (5) is not satisfied. However, we can observe from Figure 5 that a significant portion of probe packets are injected into the second link at rate higher than 50 [Mbps], regardless of the value of  $K_0$ . Also, when the incoming rate is high, the outgoing rate of probe packets tends to become smaller than the incoming rate, especially with larger  $K_0$ . These results mean that we can utilize the principle described in Subsection 2.2 to measure the available bandwidth of the second link, whereas Equation (5) is not satisfied. In Figure 6, we plot the results when  $X_1 = 50$  and  $X_2 = 30$ , where the actual available bandwidth of the first and second links are 50 [Mbps] and 70 [Mbps], respectively. We can observe the similar tendency to Figure 5 and we can expect that the measurement of the second link is possible. However, the upper limit of incoming rate is a little smaller than that in Figure 5 especially with large value of  $K_0$ , which may degrade the measurement accuracy of the second link. This is because the actual available bandwidth of the first link is 50 [Mbps], which is quite small compared with physical bandwidth (100 [Mbps]).

We next focus on the effect of  $K_0$ . In the case of small  $K_0$  (Figures 4(a), 5(a), and 6(a)), we cannot observe the stable relationship between incoming and outgoing rates of probe packets. On the other hand, too large value of  $K_0$  would results in that incoming and outgoing rates are smoothed and their difference becomes invisible, as partly observed by comparing Figures 4(b) and 4(c), Figures 5(b) and 5(c), and Figures 6(b) and 6(c). This may affect the measurement accuracy, which is confirmed in Section 4. Furthermore, larger  $K_0$  requires the larger number of probe packets to obtain enough probing samples. Thus, when we set the parameter  $K_0$ , we must consider the measurement accuracy and the amount of probe packets to obtain the measurement results.

## **3.2 Proposed Method**

We propose available bandwidth measurement method of multiple parts on an end-to-end network path based on the observations in Subsection 3.1. We first show the direction of the proposed method considering a gap between an end-to-end available bandwidth measurement of a path and the multiple parts measurement of the path. We next describe a process to measure available bandwidth of arbitrary parts of a network path. Finally, we explain the detail of a step in the measurement process.

### **3.2.1 Overview**

To measure the available bandwidth of arbitrary sections of a network path utilizing the principle shown in Section 2.2, the probe packets need to arrive at each network section at a designated rate. But, it is difficult that the sender sends probe packets to arrive at a designated rate in an arbitrary network section because the packet intervals varied due to fluctuating amount of cross traffic. For this reason, the sender sends probe packets at various rates to the receiver and estimates available bandwidth of arbitrary parts of a network path based on statistical processing. The measurement process is described as below.

1. The sender sends probe packets to the receiver at various rates, whereas an intermediate router on the path record an arrival time on probe packets as a timestamp.
2. When the probe packets arrive at the receiver, the receiver estimates the available bandwidth of each network section based on arrival and departing time of probe packets at the section.
3. If the estimations of all networks complete or the measurement with high accuracy seems to be impossible, we finish the measurement. Otherwise, we return to step 1.

In what follows, we explain the detail of steps 1 and 2.

### **3.2.2 Hop-by-Hop Timestamp of Probe Packets**

The measurement principle explained in Subsection 2.2 based on the observation of a single pair of incoming and outgoing rates of probe packets on the network. Therefore, the existing measurement methods can obtain only the available bandwidth of the bottleneck part of the network. To measure the available bandwidth of multiple network sections, we assume that the intermediate

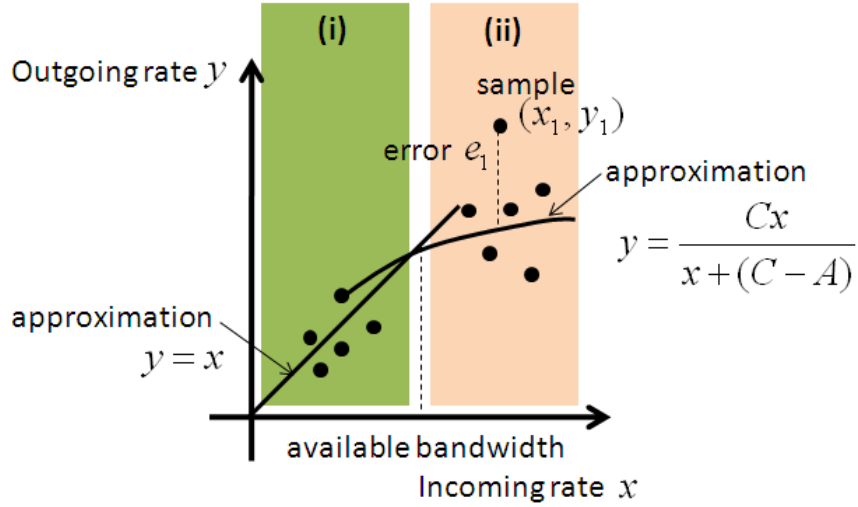


Figure 7: Computation of available bandwidth in the proposed method

routers in Figure 2 can record the times at which probe packets passing through the router. The proposed method utilizes those timestamps to estimate the available bandwidth of each network section. To my best knowledge, there is no router introduced to a real network to record times on packets, but such router is designed [38, 39] for many purposes of an end-to-end measurement.

### 3.2.3 Calculation of Available Bandwidth Based on Statistical Processing

We propose a calculation method to give the estimation result of the available bandwidth based on probing results as shown in Figure 5. The simulation results in Figure 5 can be abstracted into a simple mathematical model depicted in Figure 7. The probing results can be divided into two regions (i) and (ii). In region (i), the sending rate of probe packets is less than the actual value of the available bandwidth. Therefore, the incoming and outgoing rates become almost equal in the region. In region (ii), on the other hand, the probing packets are injected at higher rate than the actual available bandwidth. In this case the outgoing rate would be smaller than the incoming rate. We utilize a fluid model [9] to determine the outgoing rate of probe packets from incoming rates and the actual available bandwidth. We denote the incoming rate of probe packets as  $x$  [bps] and the outgoing rate of probe packets when incoming rate is  $x$  is denoted as  $y(x)$  [bps]. The physical bandwidth and the available bandwidth are denoted as  $C$  [bps] and  $A$  [bps]. Then, the model in

Figure 7 can be represented as follows.

$$y(x) = \begin{cases} x & x \leq A \\ \frac{Cx}{x+(C-A)} & x > A \end{cases} \quad (6)$$

The proposed method first gathers probing samples as in Figure 5, and determines the available bandwidth, which corresponds to  $A$  in Equation (6), by a simple regression of the equation to fit to the probing samples. This regression in the proposed method is the modified point from TOPP [40]. We explain the proposed method in detail.

The sender sends  $K$  probe packets, each of which is denoted as  $P_1, P_2, \dots, P_K$ , at a certain rate. We focus on successive  $K_0$  packets beginning with  $i$  th packet, which corresponds to  $P_i, P_{i+1}, \dots, P_{i+K_0-1}$  ( $1 \leq i \leq K - K_0 + 1$ ). We calculate the incoming and outgoing rates from timestamps at intermediate routers, which are denoted as  $x_i$  [bps] and  $y_i$  [bps], respectively. We define  $(x_i, y_i)$  as  $i$  th probing sample. Note that we can obtain  $(K - K_0 + 1)$  samples from  $K$  packets. We assume that the sender sends probing packets repeatedly, and obtains  $N_{all}$  samples. We next divide these samples based on their incoming rates to obtain average values. We set the resolution of rate to  $R_0$  [bps]. We then calculate the average value of incoming and outgoing rates of samples for each rate. We denote the averaged samples as  $(\hat{x}_k, \hat{y}_k)$  ( $1 \leq k \leq \lceil C(j)/R_0 \rceil$ ), assuming that  $C(j)$  is known in advance. We obtain the estimation results of the available bandwidth of  $j$  th network section, denoted by  $\bar{A}(j)$ , by the below equation,

$$\bar{A}(j) = \underset{A(j)}{\operatorname{argmin}} e(A(j)) \quad (7)$$

where  $e(A(j))$  is calculated as follows.

$$e(A(j)) = \sum_{\hat{x}_i \leq A(j)} (\hat{y}_i - \hat{x}_i)^2 + \sum_{\hat{x}_i > A(j)} \left( \hat{y}_i - \frac{C(j) \cdot \hat{x}_i}{\hat{x}_i + (C(j) - A(j))} \right)^2 \quad (8)$$

## 4 Performance Evaluation

We evaluate the performance of the proposed method by conducting simulation experiments using ns-2. We first evaluate the fundamental performance using 2 hop network topology including the situation where the available bandwidth of receiver-side network is larger than that of sender-side network. We next evaluate the influence of various situations for confirming the robustness of the proposed method.

### 4.1 Fundamental Evaluation of the Proposed Method

We first confirm the basic behavior of the proposed method with a simple network topology. The network topology is depicted in Figure 3, which is the same as in Subsection 3.1. In this topology, the path between the endhosts consists of the non-measuring parts and the measuring parts. The links directly connected to the endhosts on the path are not measured and the others are measured. The physical bandwidth of all links is set to 100 [Mbps]. The available bandwidth of the first link, which locates between nodes n4 and n5, is denoted as  $A(1)$ , and the available bandwidth of the second link, which locates between nodes n5 and n6, is denoted as  $A(2)$ . We vary  $A(1)$  and  $A(2)$  from 10 [Mbps] to 90 [Mbps] with 10 [Mbps] step by changing the rate of cross traffic. The timer granularity of intermediate router is set to  $1.0 \times 10^{-6}$  [s]. In this environment, we measure the available bandwidth of the second link by the proposed method.

Figure 8 exhibits the simulation results on the measurement accuracy of the available bandwidth of the second link. Each graph in Figure 8 has the different values of the actual available bandwidth of the first link ( $A(1)$ ). In each graph, we plot the relationship between actual and estimated values of the available bandwidth of the second link in cases of  $K_0 = 2, 4, 8, 16, 32$  and 47. The parameters  $K$  and  $R_0$  of the proposed method are set to 50 and 1 [Mbps]. The center of the error bars in the graph indicates the average of the estimation results, and the width of that indicates 95% confidence interval.

These figures indicate that the available bandwidth at the second link is measured accurately regardless of actual values of available bandwidth of two links ( $A(1)$  and  $A(2)$ ). Especially when  $A(2) < A(1)$ , which satisfies Equation (5), the available bandwidth is measured with high accuracy. On the other hand, when  $A(2) > A(1)$ , which does not satisfy Equation (5), the measurement accuracy remains reasonable. However, especially when  $A(2)$  becomes close to 100 [Mbps], the

measurement accuracy degrades especially when  $A(1)$  is small. This is because of the decrease in the number of probing results whose incoming rate is larger than  $A(2)$ . We can also observe from Figure 8 that to obtain accurate measurement results we should avoid from setting  $K_0 = 2$  since the measurement results have significant fluctuations. This is because the relationships between incoming and outgoing rates become unstable, as shown in Figures 4(a), 5(a), and 6(a).

## 4.2 Influence of Physical Bandwidth

We evaluate the influence of physical bandwidth on measurement accuracy with the same network topology as the previous simulation experiments. The difference from the previous experiments are values of the physical bandwidth and the available bandwidth of all links in the network. The physical bandwidth is set to 10 [Mbps] and 1 [Gbps]. The cross traffic rates and available bandwidths are configured proportionally to the physical bandwidth.

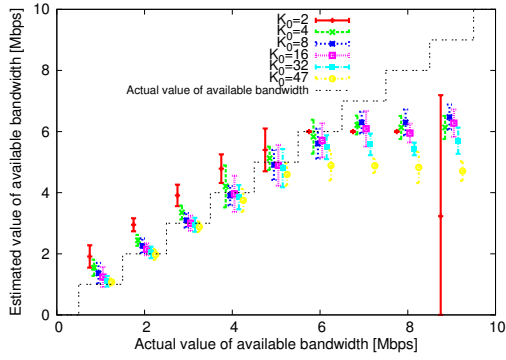
Figures 9 and 10 exhibit the simulation results of available bandwidth of the second link where the physical bandwidth is set to 10 [Mbps] and 1 [Gbps], respectively. We focus on the measurement results of the same bandwidth utilization of both the first and the second links in Figures 8, 9, and 10. These figures indicate that the available bandwidth can be measured accurately regardless of the physical bandwidth. In general, when the physical bandwidth is large, the measurement accuracy becomes low because of timer granularity of intermediate router. However, in the proposed method, the statistical processing can compensate the measurement accuracy.

## 4.3 Influence of Hop Count of a Path

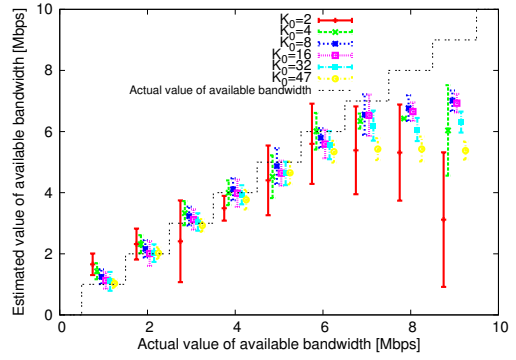
We next evaluate the influence of the hop count of a path on the measurement accuracy. We first utilize 3 hop topology to confirm the performance of the proposed method in detail. After that, we utilize 3, 5, and 9 hop topologies to evaluate the influence of the hop count on the measurement accuracy.

We first present the simulation results with three hop topology depicted in Figure 11. The probe packets are sent from node  $n_0$  to node  $n_2$ . The cross traffic is sent from node  $n_1$  to node  $n_9$ , from node  $n_8$  to node  $n_{11}$ , and from node  $n_{10}$  to node  $n_3$ . The available bandwidth of the first link, which locates between nodes  $n_4$  and  $n_5$ , is denoted as  $A(1)$ , that of the second link, which locates between nodes  $n_5$  and  $n_6$ , is denoted as  $A(2)$ , and that of the third link, which located

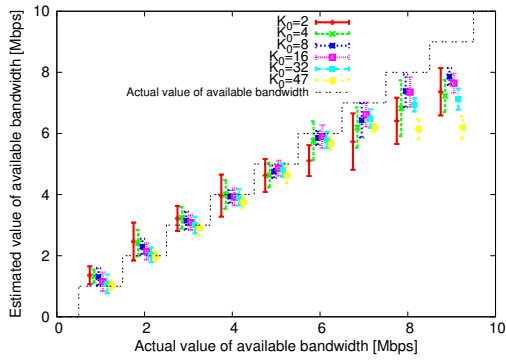




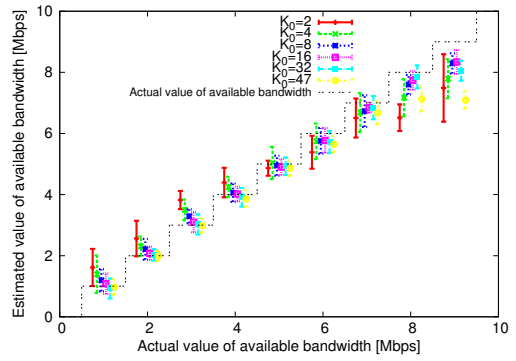
(a)  $A(1) = 1$  [Mbps]



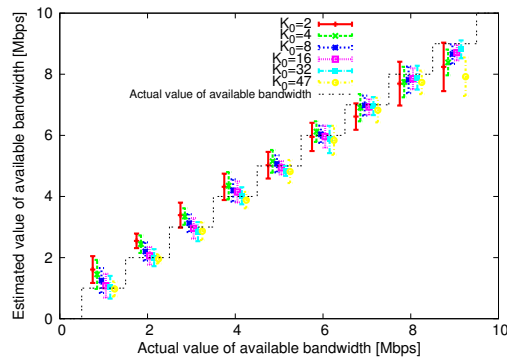
(b)  $A(1) = 3$  [Mbps]



(c)  $A(1) = 5$  [Mbps]



(d)  $A(1) = 7$  [Mbps]



(e)  $A(1) = 9$  [Mbps]

Figure 9: Estimation results with 10 [Mbps] of physical bandwidth

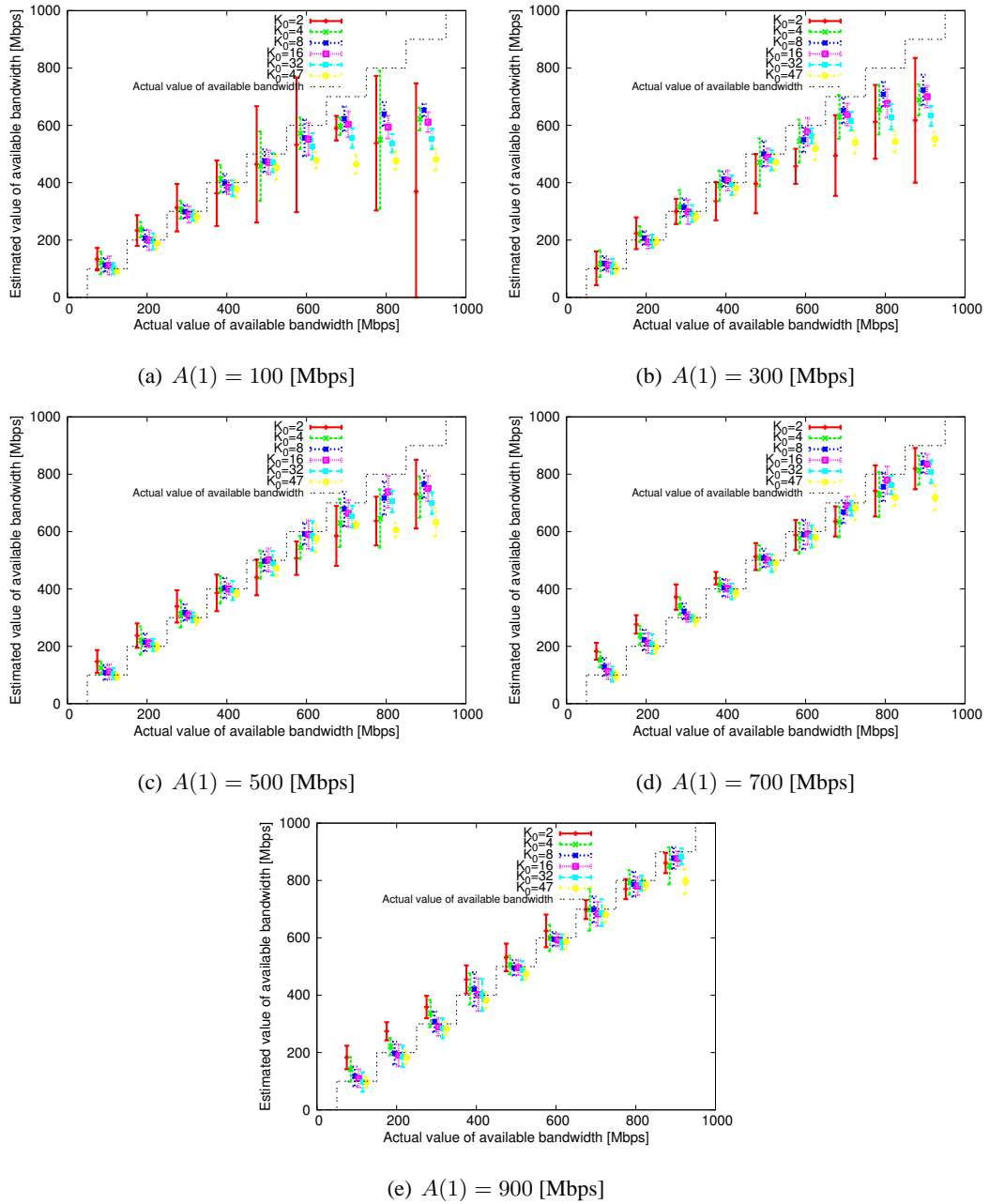


Figure 10: Estimation results with 1 [Gbps] of physical bandwidth

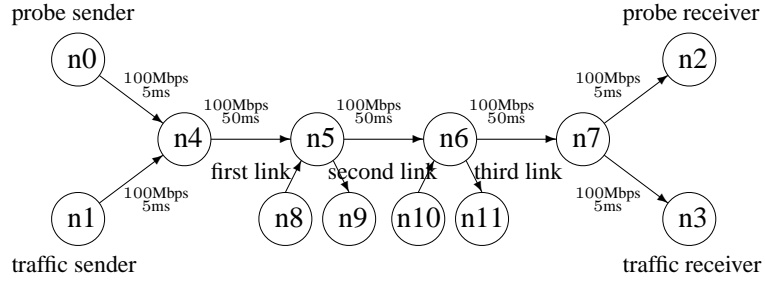


Figure 11: 3 hop network topology

between nodes n6 and n7, is denoted as  $A(3)$ . We vary  $A(1)$ ,  $A(2)$ , and  $A(3)$  from 10 [Mbps] to 90 [Mbps] with 20 [Mbps] step by changing the rate of cross traffic. In the environment, we assess the measurement accuracy of the available bandwidth of the third link, depending on the cross traffic on the first and second links.

The measurement results of the available bandwidth of the third link are presented in Figures 12–16. Each figure has a different available bandwidth of the first link. The figures indicate that in the case where the available bandwidth of the third link is smaller than both the first link and the second link, which satisfies Equation (5), the available bandwidth of the third link is measured with high accuracy. Furthermore, in the case where the available bandwidth of the third link is larger than either the first link or the second link, which does not satisfy Equation (5), the measurement accuracy remains reasonable.

We next discuss about the influence of  $K_0$  on measurement accuracy. In the case where the available bandwidth of the third link is smaller than both that of the first link and the second link, which satisfies Equation (5), the high measurement accuracy is obtained when a value of  $K_0$  is large, such as  $K_0 = 32, 47$ . This is because relationships between incoming and outgoing rates of probe packets becomes similar to the fluid model due to smoothing incoming and outgoing rates by increasing the number of probe packets to be utilized. Meanwhile, in the case where the available bandwidth of the third link is larger than either that of the first or the second link, which does not satisfy Equation (5), the measurement accuracy with  $K_0 = 8, 16$  is higher than those with  $K_0 = 32, 47$ . The reason for this is that when the value of  $K_0$  is too large, the incoming rate of probe packets at the third link cannot become higher than the actual available bandwidth of the third link. On the other hand, when the value of  $K_0$  is too small, the available bandwidth cannot be measured accurately due to the same reason as in Figure 8.

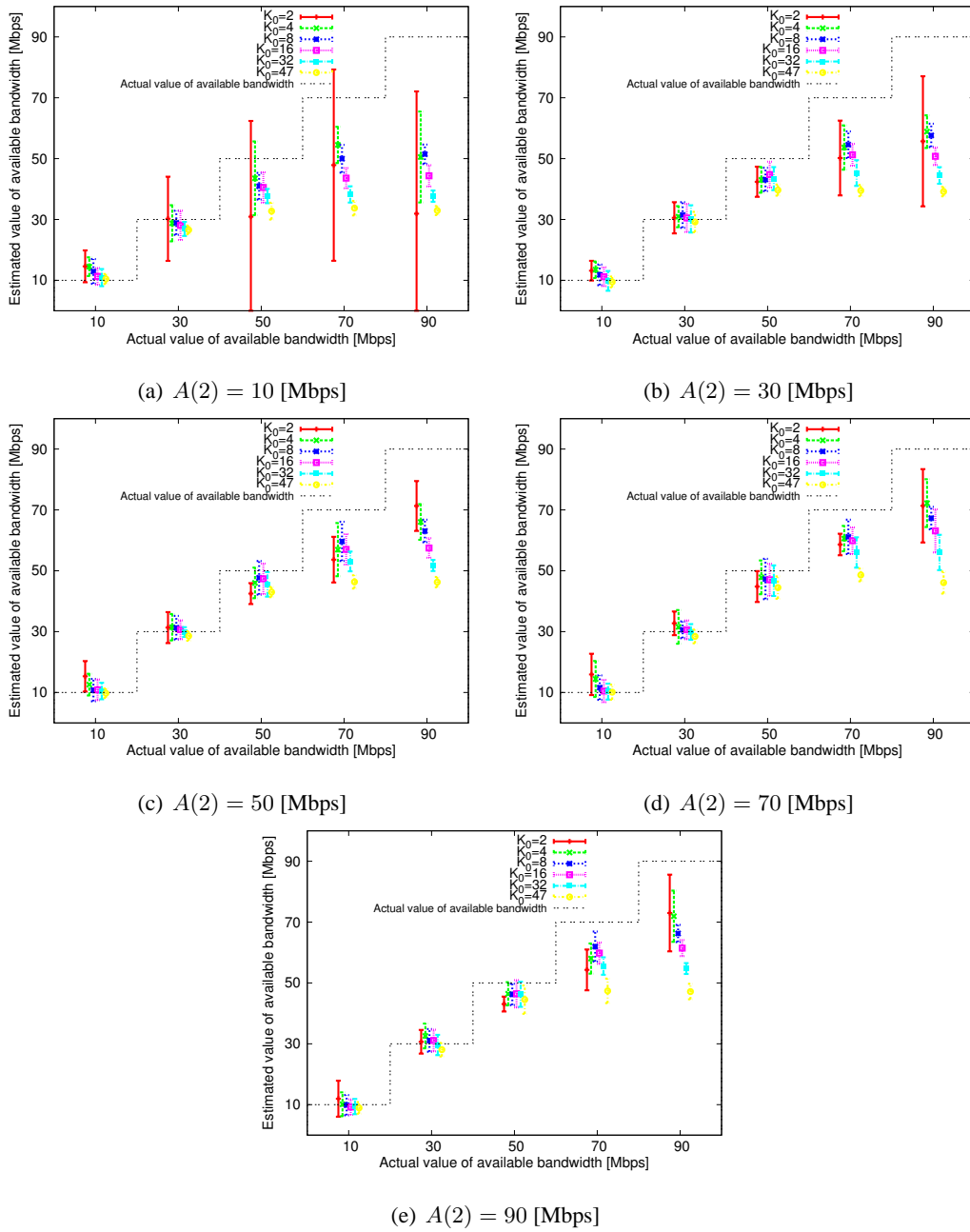
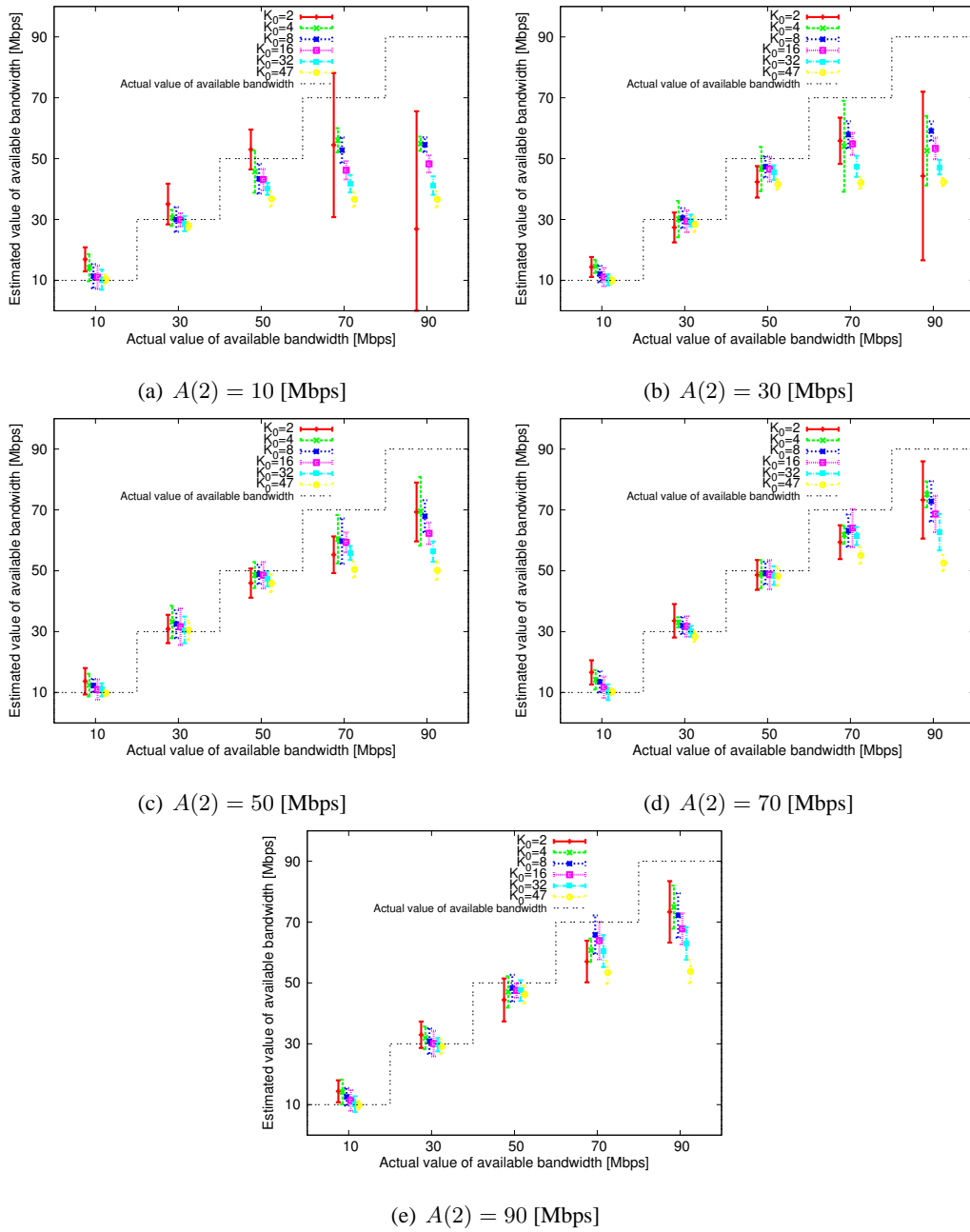
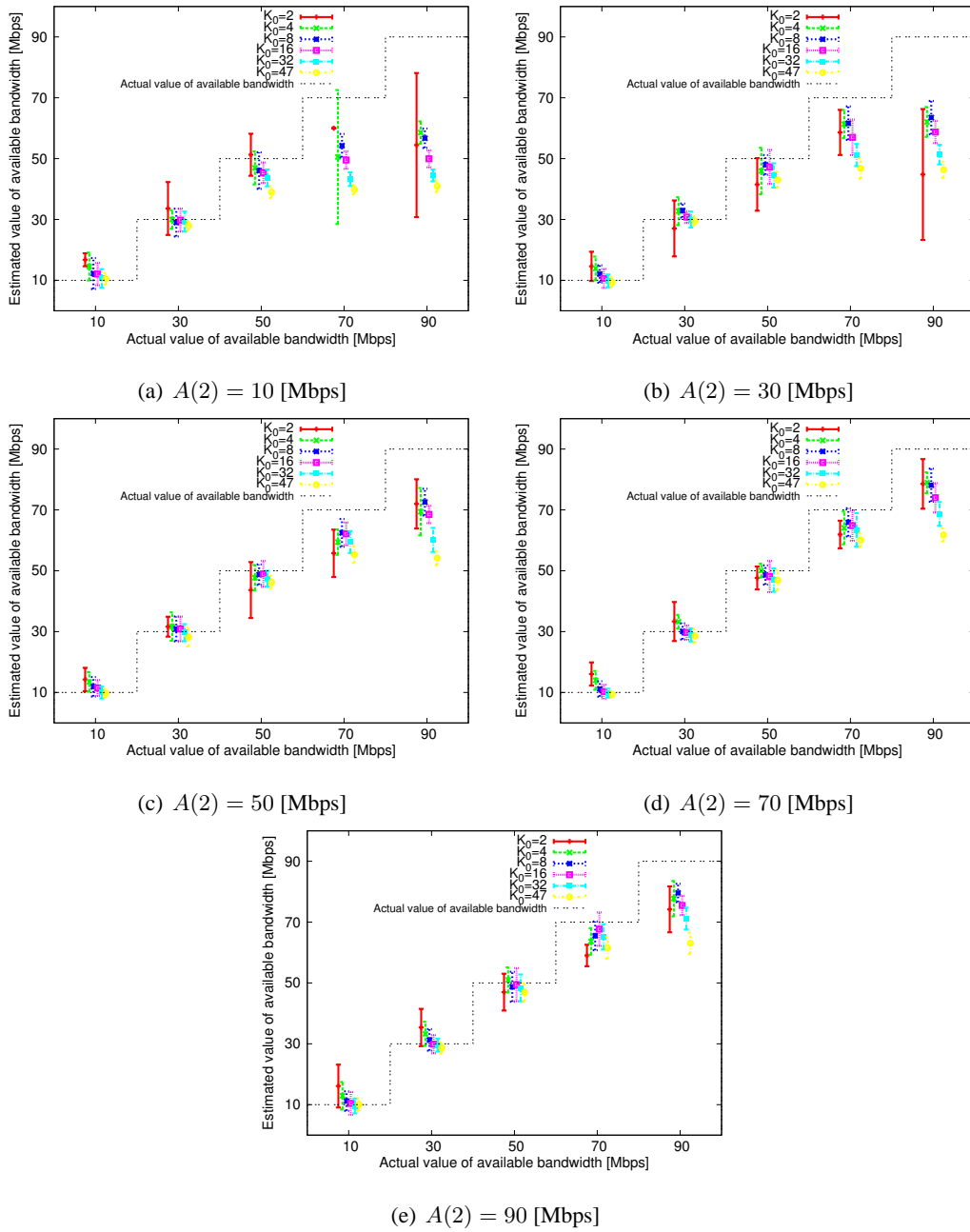


Figure 12: Estimation results with 3 hop topology when  $A(1) = 10$  [Mbps]





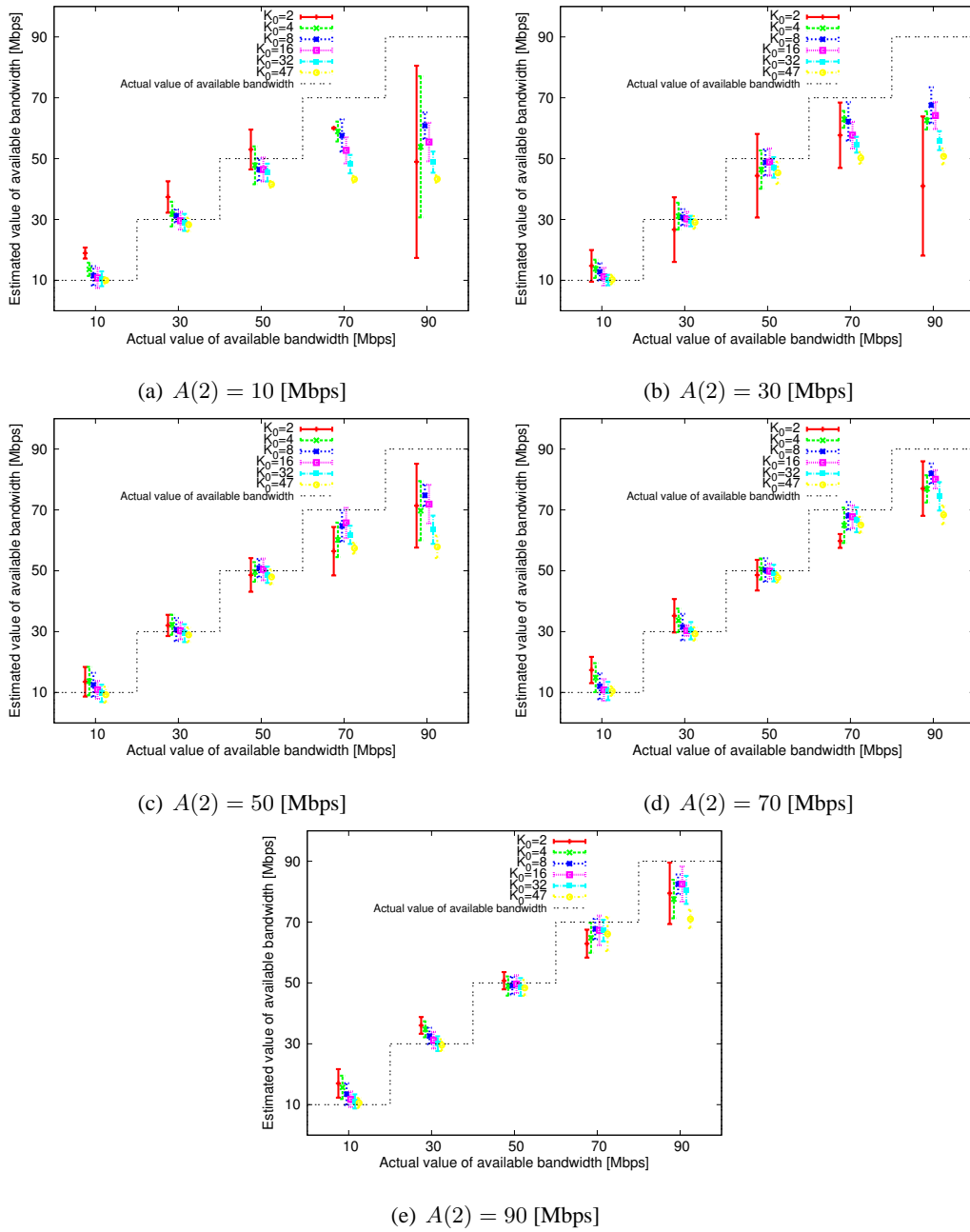


Figure 15: Estimation results with 3 hop topology when  $A(1) = 70$  [Mbps]

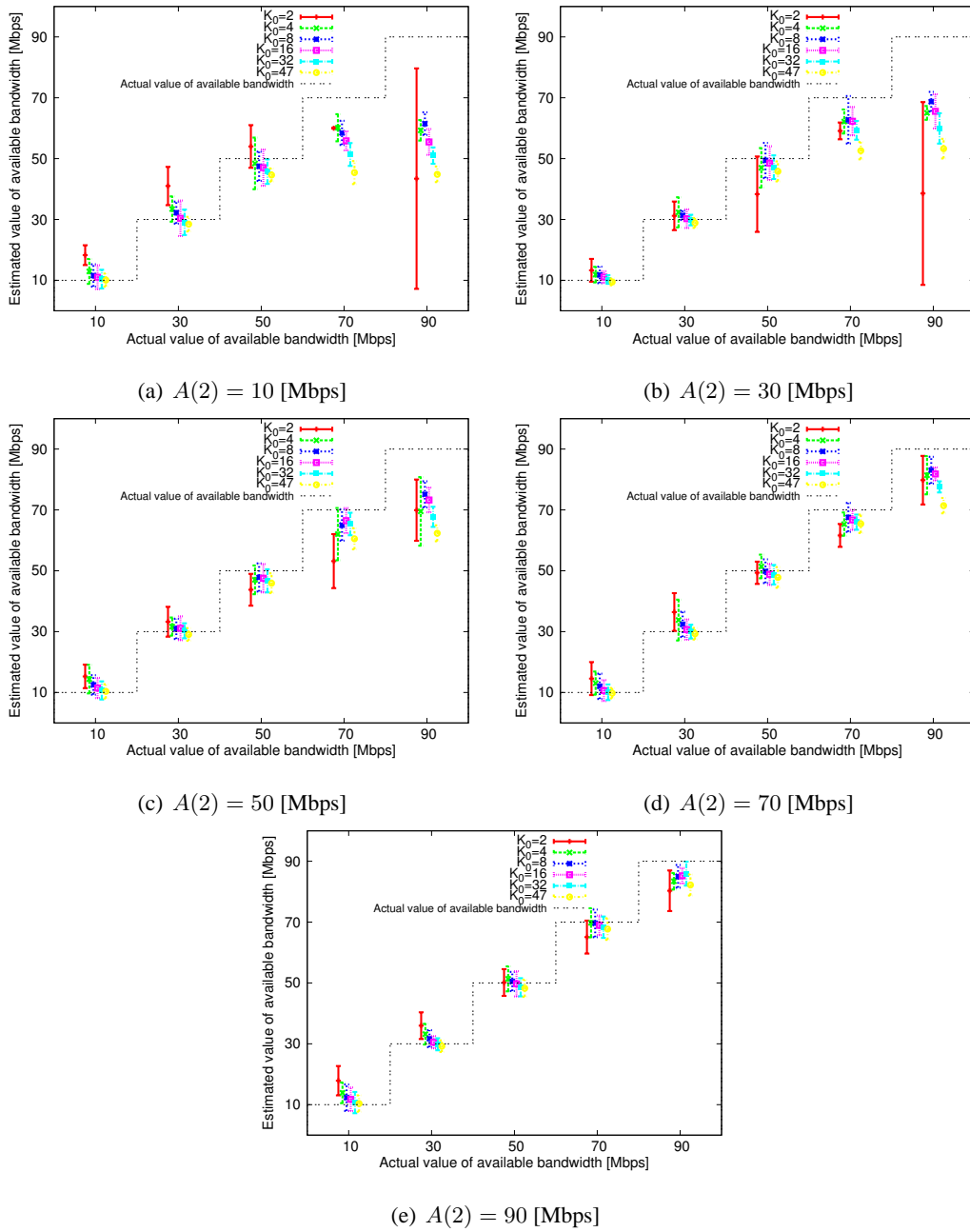


Figure 16: Estimation results with 3 hop topology when  $A(1) = 90$  [Mbps]

We next focus on Figures 13(d) and 15(b). Figure 13(d) indicates the measurement result when the available bandwidth of the first link and the second link is 30 and 70 [Mbps]. In this case, the bandwidth bottleneck in this environment is located at the first link. On the other hand, the bandwidth bottleneck in the environment in Figure 15(b) is located at the second link. In both cases, the available bandwidth of the bottleneck link is 30 [Mbps]. By comparing these figures, we observe that the available bandwidth of the third link is measured accurately when the bottleneck location is the first link compared with the case when that is the second link. This is because when the bandwidth bottleneck is located at the first link, the number of probe packets with high rates increases due to the changes in cross traffic at the second link. On the other hand, when the bottleneck is located at the second link, the number of probe packets with high rates is small because the outgoing rate from the second link becomes small due to the small available bandwidth of the second link.

We next evaluate the influence of the hop count of the path on the measurement accuracy utilizing the network topologies depicted in Figure 17. From the previous results, we found that the measurement accuracy mostly depends on whether Equation (5) is satisfied or not. For this reason, we utilize following two cross traffic scenarios.

**Scenario 1** From the sender host to receiver host, the available bandwidth decreases gradually with identical gaps.

**Scenario 2** From the sender host to receiver host, the available bandwidth increases gradually with identical gaps.

The detailed setting of the available bandwidth is summarized in Table 1. The estimation results are shown in Figures 18 and 19 for Scenario 1 and 2, respectively. Each graph in the figures has different hop count of the path. Figure 18 indicates that when the available bandwidth becomes smaller as the hop count from the sender host increases, which satisfies Equation (5), the available bandwidth can be measured accurately regardless of the total number of hop counts between the sender and the receiver. However, Figure 19 indicates that in the opposite case, which does not satisfies Equation (5), the estimation accuracy becomes worse as the hop count from the sender increases. This is because when probe packets traverse multiple links with smaller available bandwidth, their incoming rates in the following network sections becomes smaller with higher probability.

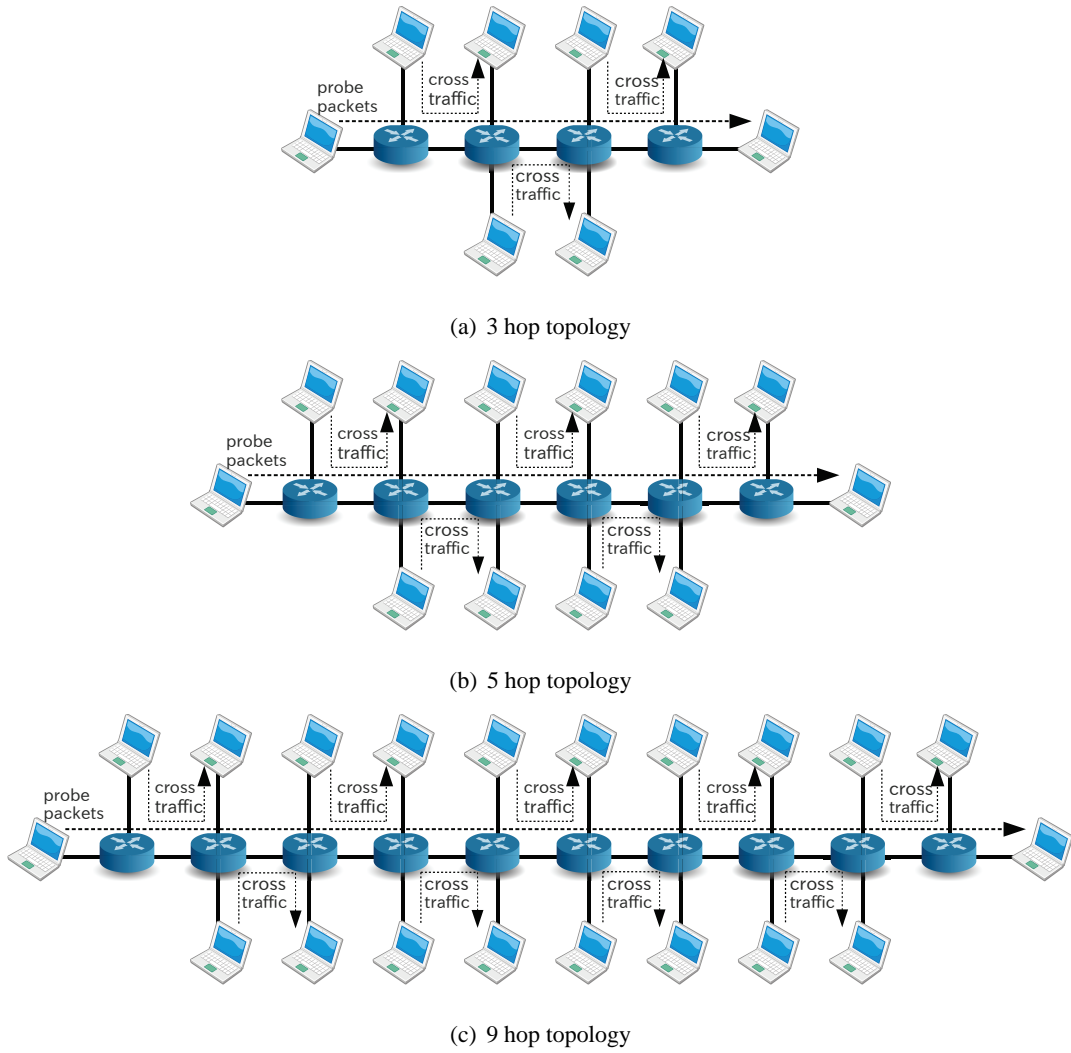
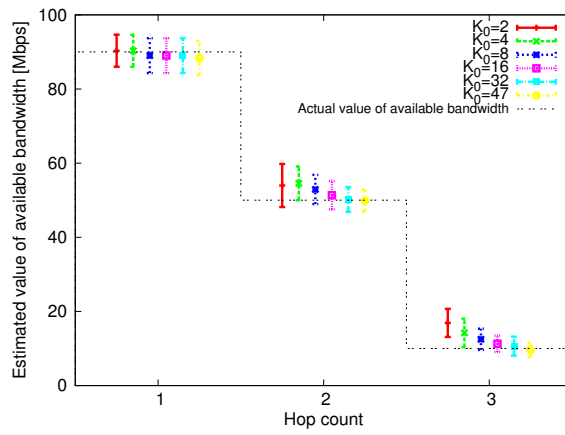


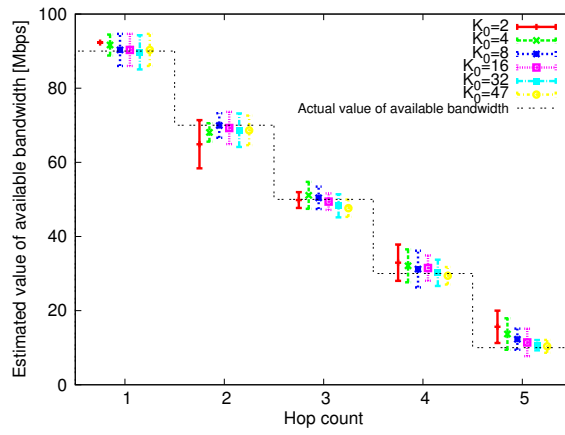
Figure 17: Network topologies with longer hop counts

Table 1: Settings of available bandwidth in 3, 5, and 9 hop topologies

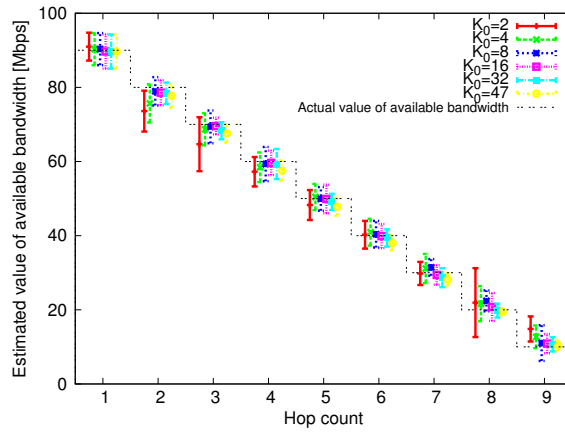
	scenario 1	scenario 2
3 hop topology	(90, 50, 10) [Mbps]	(10, 50, 90) [Mbps]
5 hop topology	(90, 70, 50, 30, 10) [Mbps]	(10, 30, 50, 70, 90) [Mbps]
9 hop topology	(90, 80, 70, ..., 10) [Mbps]	(10, 20, 30, ..., 90) [Mbps]



(a) 3 hop network

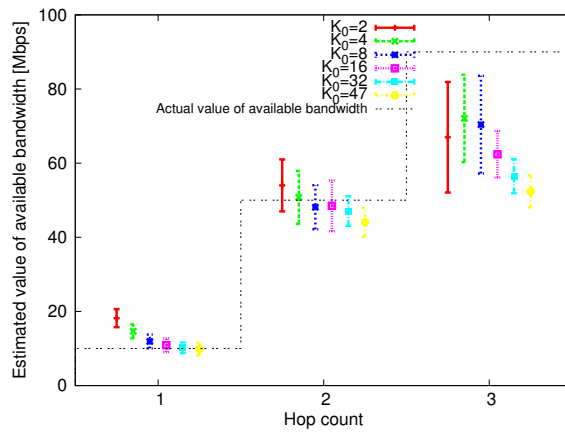


(b) 5 hop network

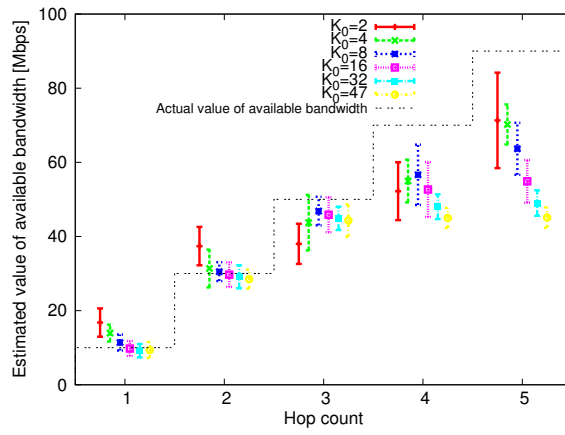


(c) 9 hop network

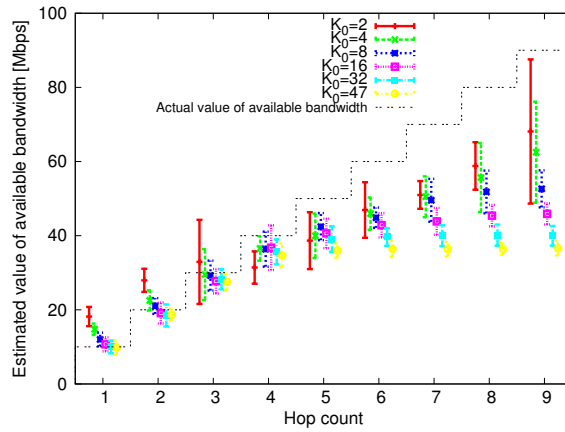
Figure 18: Effect of hop count in scenario 1



(a) 3 hop network



(b) 5 hop network



(c) 9 hop network

Figure 19: Effect of hop count in scenario 2

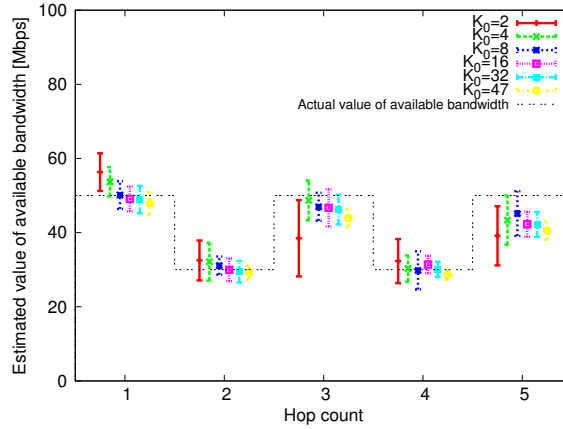


Figure 20: Estimation results in multiple bottleneck situation

#### 4.4 Performance in multiple bottleneck situation

We finally verify the performance of the proposed method in the situation when there are multiple bottleneck locations on the path. We utilize 5 hop network topology depicted in Figure 17(b). The physical bandwidth of the links is set to 100 [Mbps] and the available bandwidth of each link from the sender is 50, 30, 50, 30, and 50 [Mbps]. The estimation results are depicted in Figure 20. The figure indicates that all links of the path are measured accurately and the bottleneck locations of the path are specified successfully from the estimation results. This means that we can specify the bottleneck locations of a path utilizing the proposed method regardless of the number of the bottleneck locations.

## **5 Conclusion and Future Work**

In this thesis, we proposed the simultaneous measurement method of multiple parts on an end-to-end network path. We extend the measurement principle utilized in existing measurement tools by adding a small function to intermediate routers on the path. We validated the performance of the proposed method by simulation experiments and obtained the results that the available bandwidth of multiple parts of the path can be measured with reasonable accuracy even when the available bandwidth of receiver-side network is larger than that of sender-side network. We also validated the robustness of the proposed method in various situations.

In future work, we plan to introduce the algorithm to configure the number of probe packets to decrease the measurement load on the network, while keeping the measurement accuracy. Furthermore, we need to implement the proposed method and verify the effectiveness of the proposed method in actual network environment.

## **Acknowledgments**

I appreciate many people related not only to my research but also to my life in our laboratory.

First, I would like to express sincere gratitude to my supervisor Professor Masayuki Murata of Osaka University. My research cannot be achieved without his significant advices.

I would like to express my sincere appreciation to Associate Professor Go Hasegawa of Osaka University. His advices gave me breakthrough of some difficulties of my research and his guidance led me to make a growth as a person.

I would like to appreciate to Professor Naoki Wakamiya, Associate Professor Shin'ichi Arakawa and Assistant Professor Yuichi Ohsita of Osaka University for valuable comments and advices for my research.

I appreciate my colleague in Murata Laboratory. They give me the best environment to work comfortably and efficiently. Furthermore, they give me valuable ideas for my research.

## References

- [1] “Hobbes’ Internet Timeline.” available at <http://www.zakon.org/robert/internet/timeline/>.
- [2] J. Kim, J. Yun, M. Yoon, K. Cho, H. Lee, and K. Han, “A Routing Metric Based on Available Bandwidth in Wireless Mesh Networks,” in *Proceedings of ICACT 2010*, pp. 844–849, February 2010.
- [3] C. L. T. Man, G. Hasegawa, and M. Murata, “ImTCP: TCP with an Inline Measurement Mechanism for Available Bandwidth,” *Computer Communications Journal Special Issue of Monitoring and Measurements of IP Networks*, vol. 29, no. 10, pp. 2469–2479, June 2006.
- [4] E. Ko, D. An, and I. Yeom, “Dealing with Sudden Bandwidth Changes in TCP,” in *Proceedings of ICC 2008*, pp. 3007–3011, May 2008.
- [5] C. Robert L and M. E. Crovella, “Dynamic Server Selection using Bandwidth Probing in Wide-Area Networks,” tech. rep., Boston University, 1996.
- [6] M. Jain and C. Dovrolis, “End-to-End Available Bandwidth: Measurement Methodology, Dynamics, and Relation with TCP Throughput,” in *Proceedings of ACM SIGCOMM 2002*, pp. 295–308, August 2002.
- [7] V. J. Ribeiro, R. H. Riedi, R. G. Baraniuk, J. Navratil, and L. Cottrell, “pathChirp: Efficient Available Bandwidth Estimation for Network Paths,” in *Proceedings of PAM 2003*, pp. 1–11, April 2003.
- [8] C. L. T. Man, G. Hasegawa, and M. Murata, “ICIM: An Inline Network Measurement Mechanism for Highspeed Networks,” in *Proceedings of the E2EMON 2006*, pp. 66–73, April 2006.
- [9] J. Strauss, D. Katabi, and F. Kaashoek, “A Measurement Study of Available Bandwidth Estimation Tools,” in *Proceedings of IMC 2003*, pp. 39–44, October 2003.
- [10] A. B. Downey, “Using Pathchar to Estimate Internet Link Characteristics,” in *Proceedings of ACM SIGCOMM 1999*, pp. 241–250, October 1999.

- [11] N. Hu and P. Steenkiste, "Evaluation and Characterization of Available Bandwidth Probing Techniques," *IEEE Journal on Selected Areas in Communications*, vol. 21, no. 6, pp. 879–894, August 2003.
- [12] J. Navratil and R. L. Cottrell, "ABwE: A Practical Approach to Available Bandwidth Estimation," in *Proceedings of PAM 2003*, pp. 1–5, April 2003.
- [13] E. Bergfeldt, S. Ekelin, and J. M. Karlsson, "Real-time Available-Bandwidth Estimation using Filtering and Change Detection," *Computer Networks*, vol. 53, no. 15, pp. 2617–2645, October 2009.
- [14] M. Jain and C. Dovrolis, "End-to-End Estimation of the Available Bandwidth Variation Range," in *Proceedings of SIGMETRICS 2005*, pp. 265–276, June 2005.
- [15] L. Lao, C. Dovrolis, and M. Y. Sanadidi, "The Probe Gap Model can Underestimate the Available Bandwidth of Multihop Paths," *ACM SIGCOMM Computer Communication Review*, vol. 36, no. 5, pp. 29–34, October 2006.
- [16] X. Hei, B. Bensaou, and D. H. K. Tsang, "Model-based End-to-End Available Bandwidth Interference using Queueing Analysis," *Computer Networks*, vol. 50, no. 12, pp. 1916–1937, August 2006.
- [17] A. Shriram, M. Murray, Y. Hyun, N. Brownlee, A. Broido, M. Fomenkov, and K. Claffy, "Comparison of Public End-to-End Bandwidth Estimation Tools on High-Speed Links," in *Proceedings of PAM 2005*, pp. 306–320, March 2005.
- [18] C. Tang and P. K. McKinley, "On the Cost-Quality Tradeoff in Topology-Aware Overlay Path Probing," in *Proceedings of ICNP 2003*, pp. 268–279, November 2003.
- [19] S. Ekelin, M. Nilsson, E. Hartikainen, and A. Johnsson, "Real-Time Measurement of End-to-End Available Bandwidth using Kalman Filtering," in *Proceedings of IEEE/IFIP NOMS 2006*, pp. 73–84, April 2006.
- [20] N. Hu, L. E. Li, Z. M. Mao, P. Steenkiste, and J. Wang, "Locating Internet Bottlenecks: Algorithms, Measurements, and Implications," in *Proceedings of ACM SIGCOMM 2004*, pp. 41–54, September 2004.

- [21] X. Xing and S. Mishra, "Where is the Tight Link in a Home Wireless Broadband Environment?," in *Proceedings of ASCOT 2009*, pp. 1–10, September 2009.
- [22] D. Gupta, D. Wu, P. Mohapatra, and C.-N. Chuah, "Experimental Comparison of Bandwidth Estimation Tools for Wireless Mesh Networks," in *Proceedings of IEEE INFOCOM 2009*, pp. 2891–2895, April 2009.
- [23] A. Johnsson and M. Bjorkman, "On Measuring Available Bandwidth in Wireless Networks," in *Proceedings of LCN 2008*, pp. 861–868, October 2008.
- [24] E. Bergfeldt, S. Ekelin, and J. M. Larlsson, "A Performance Study of Bandwidth Measurement Tools over Mobile Connections," in *Proceedings of VTC Spring 2009*, pp. 1–5, April 2009.
- [25] A. Amamra and K. M. Hou, "Available Bandwidth Estimation in Wireless Ad Hoc Network: Accuracy and Probing Time," in *Proceedings of CSE 2008*, pp. 379–387, July 2008.
- [26] C. D. Guerreo and M. A. Labrador, "A Hidden Markov Model Approach to Available Bandwidth Estimation and Monitoring," in *Proceedings of INM 2008*, pp. 1–6, October 2008.
- [27] L. He, B. Tang, and S. Yu, "Available Bandwidth Estimation and its Application in Detection of DDoS Attacks," in *Proceedings of ICCS 2008*, pp. 1187–1191, November 2008.
- [28] H. Wang, L. Gao, and Z. Li, "Node-to-Node Available Bandwidth Estimation in Ad Hoc Networks," in *Proceedings of ICCEE 2008*, pp. 701–705, December 2008.
- [29] T. G. Sultanov and A. M. Sukhov, "Simulation Technique for Available Bandwidth Estimation," in *Proceedings of EMS 2010*, pp. 490–495, November 2010.
- [30] N. Sundaram and P. Ramanathan, "M-Perf: An Available Bandwidth Estimation Tool for Multicast Applications," in *Proceedings of Allerton 2008*, pp. 170–176, September 2008.
- [31] X. Liu, K. Ravindran, and D. Loguinov, "A Queueing-Theoretic Foundation of Available Bandwidth Estimation: Single-Hop Analysis," *IEEE/ACM Transactions on Networking*, vol. 15, no. 4, pp. 918–931, August 2007.

- [32] C. U. Castellanos, D. L. Villa, O. M. Teyeb, J. Elling, and J. Wigard, "Comparison of Available Bandwidth Estimation Techniques in Packet-Switched Mobile Networks," in *Proceedings of PIMRC 2006*, pp. 1–5, September 2006.
- [33] H. Esaki and H. Kan, "Dynamic Traffic Load Balancing Mechanism for SHAKE Architecture," in *Proceedings of WIRELESSCOM 2005*, pp. 636–640, June 2005.
- [34] "Qik — Record and share video live from your mobile phone." available at <http://qik.com>.
- [35] "Free Skype internet calls and cheap calls to phones online - Skype." available at <http://www.skype.com/intl/en/home>.
- [36] "ns-2 web page." available at <http://isi.edu/nsnam/ns/>.
- [37] C. Dovrolis, P. Ramanathan, and D. Moore, "What do Packet Dispersion Techniques Measure?," in *Proceedings of INFOCOM 2001*, vol. 2, pp. 905–914, April 2001.
- [38] A. Machizawa, H. Toriyama, T. Iwama, and A. Kaneko, "Development of a Cascadable Passing Through Precision UDP Time-Stamping Device," *IEICE Transactions on Communications*, vol. J88-B, no. 10, pp. 2002–2011, October 2005. (in Japanese).
- [39] A. Machizawa and Y. Kitaguchi, "Improvement of Software Timestamp Accuracy with Interrupt Handler and High Precision PC," *IEICE Transactions on Communications*, vol. J87-B, no. 10, pp. 1678–1685, October 2004. (in Japanese).
- [40] B. Melander, M. Bjorkman, and P. Gunningberg, "A New End-to-End Probing and Analysis Method for Estimating Bandwidth Bottlenecks," in *Proceedings of GLOBECOM 2000*, vol. 1, pp. 415–421, November 2000.